CRITICAL STRAIN PERFORMANCE OF COATING SYSTEMS AT AIRCRAFT JOINTS

Ung Hing Tiong, Graham Clark
School of Aerospace, Mechanical and Manufacturing Engineering, RMIT University
Bundoora, Victoria, Australia
in conjunction with
Defence Materials and Technology Centre, Hawthorn, Victoria, Australia

Abstract

Aircraft protective coatings are primarily used to protect structural elements from a corrosive environment. The durability of these coatings is a primary concern, since environmental degradation from moisture, high temperature, ultraviolet radiation and chemical factors can significantly reduce the effective service lifetime of paints and sealants. The magnitude of applied loads and the effect of load history are also likely to be contributors to the process of coating degradation. This aspect of work so far has received little attention in the literature. This paper describes the key characteristics of coatings at aircraft joints. Of particular interest are the sites where movement is concentrated at joints – sites such as exposed sheet ends and fastener heads, which are therefore likely to be susceptible to enhanced coating cracking. This represents a step in assessing the contribution of the complex strain history at an aircraft joint as part of developing a prognostic capability for the service life of aircraft coatings. In this study, the results from displacement analysis on two different lap joints are used to estimate the coating strain likely to be experienced at the paint/sealant bead. Ongoing work will consider modelling of actual coating and sealant in the system.

1 Introduction

External military aircraft coating schemes currently adopted by most Australian Defence Force aircraft, are based on a chromate pretreatment, an epoxy primer and a polyurethane topcoat. The entire coating system is quite thin ie. 50 to 125 micrometres. The internal paint scheme is usually primer, but with extensive use of sealants in some areas. Each layer performs several special functions and interacts with other layers to achieve overall coating system performance. For example, the epoxy primers are adherent and usually contain inhibitors which will retard corrosion of the underlying substrate once the coating is breached. The polyurethane topcoat is resistant to weather and chemicals, flexible and provides the desired appearance. A sealant coat is often applied at faying surfaces, exposed sheet ends and around fastener holes to help maintain flexibility of the coating system and prevent penetration of joints by the environment or fuels. The topcoat may have a shorter service life than internal schemes because of the need to repaint to maintain appearance.

Current aircraft coating systems have been subject to extensive refinement, and if correctly applied, perform well. However, several types of location in airframes are particularly susceptible to coating failure, and attract increased maintenance attention; these locations are typically at mechanically fastened joints which can exhibit substantial displacement under service loads. Corrosion is observed to be focused in these areas [1]. This has been highlighted in accidents like the Aloha B737 accident [2], which involved corrosion-related cracking at fuselage joints. Visual inspection for such damage is impossible without stripping the paints, removing the rivets and opening the joints.

A review by Furuta et al. [3] noted that joint specimens subjected to a corrosive environment during cyclic loading exhibited fatigue lives 30-50% shorter than those tested in an ambient temperature. Developing and understanding ways to improve the durability of corrosion protection around joint is therefore highly desirable in terms of managing corrosion in ageing aircraft. Clark [4], in discussing the impact of corrosion on structural life, explicitly noted that the overall service life of a corroded part is critically sensitive to the life of protective coatings. As a result the development of prognostic tools for the service life of coatings, under realistic service conditions, represents an important goal which requires an understanding of the various parameters which can influence the coating degradation processes and rate.

Mechanical and material modelling of in-service paint/sealant applied around the structural joints is expected to be important in estimating coating life. The present study considers the structural modelling aspect, and future work in conjunction with University of Queensland will extend the modelling to include paint/sealant in the system, focussing on thermomechanical degradation of these components, SEM analysis of paint degradation, as well as fatigue crack growth modelling in the coating system.

This part of the work contributes to a larger research program, which will develop tools for predicting the impact of real service environment (thermomechanical) on coating longevity for military aircraft in Australia. Such tools will be particularly useful in estimating the residual strength or service life of paint system at stress concentrations associated with joints, because of the difficulties in detecting the occurrence of corrosion in such locations.

2 Coating Failure Environment

Coating degradation research has concentrated primarily on two major weathering factors, namely (i) ultraviolet (UV) radiation exposure and (ii) the combined effect of heat and moisture (the hydrothermal effect) [5-7]. The polyurethane topcoat degradation is influenced by UV, while UV has little effect on the underlying epoxy primer. In contrast, the hydrothermal effect exerts a detrimental influence on both topcoat and primer. In general, these environmental exposures promote a series of chemical reactions in the polyurethane topcoat, with progressive deterioration in coating mechanical properties; the process can be accelerated by the presence of water and elevated temperature. Polyurethane topcoat deterioration can be measured through changes in coating appearance and coating mechanical properties such as tensile strength, elongation, impact strength and elastic modulus [8]. Discoloration, embrittlement, tackiness, loss of surface gloss, crazing or chalking of the surface [9] are effects commonly observed in terms of appearance.

Skaja et al. [10] and Guo et al. [11] suggested that a significant increase in the elastic modulus of the coating surface was related to the formation of oxidative products. Various surface analysis techniques, such as atomic force microscopy (AFM), X-ray photoelectron spectroscopy (XPS), Fourier transform infra-red spectroscopy (FTIR) and scanning electron microscopy (SEM) techniques are available for monitoring degradation; Yang et al. [12] monitored polyurethane topcoat in a test chamber using these methods, and discovered the formation of blisters on the coating surface during the early stage of degradation process. The blistering increased in concentration and size at longer UV exposure times, and there was subsequent micro-cracking and loss of coating gloss as a result of local blister breakage [13].

Popov et al. [14] observed that residual stresses have exactly same effect as externally applied stresses, in that they accelerate the ageing process. White and Turnbull [15] noted that while applied tensile stress on a coating in the presence of UV and oxygen accelerated the coating ageing process, a compressive stress would often retard the process. This suggests a key role of mechanical stress in promoting degradation in the form of cracking.

Research has focused predominantly on chemical and physical ageing/degradation of polyurethane coating. The role of applied mechanical stain as a contributory part of the overall environmental coating degradation model has received little attention so far, particularly at strain concentrations associated with joints.

Some regions in aircraft structural joints can move significantly under service loads, and the joint effectively concentrates that displacement into discrete locations such as exposed sheet ends and fastener head locations (see the example in Figure 1).

Joint movement is made up of two specific components; one is shear displacement resulting from the overall in-plane stressing and the differences in the deformation of the loaded and unloaded parts of the joint. The other displacements result from geometrical eccentricities in the joint, appearing as out-of-plane deformation and separation of sheet ends. These movements will lead to distortion, elongation or bending of any applied coating system. This paper describes an assessment of the strain likely to be experienced by a coating material at some locations in generic joint configurations.

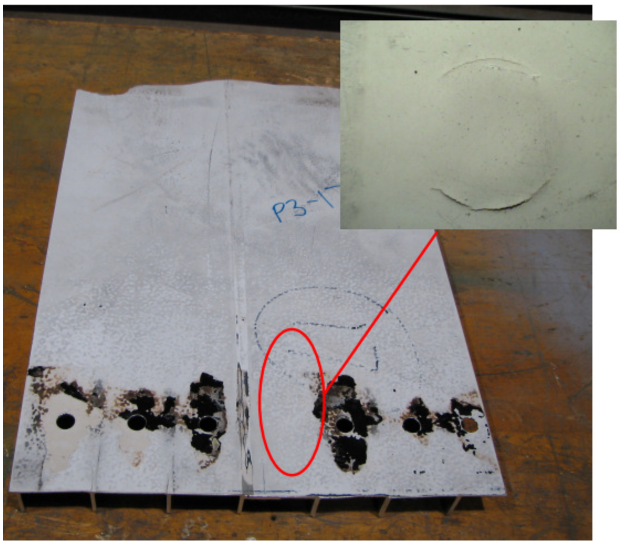

Figure 1 Cracking of protective coatings around fastener head (insert) in a retired military aircraft wing panel

3 Joint Configurations and Finite Element Analysis

Two types of lap joint were selected for this study. The joints differed in geometrical profiles, sheet thickness, overlapping area, edge distance, alloy and load distribution, and this study investigated the displacements expected at the joint sheet ends – expected to be prime sites for coating failure. The type of fastener head used differed; one joint used dome-head fasteners normally found in internal structure, while the other used countersunk fasteners, corresponding to an application on an external surface where a clean profile is required.

3.1 Dome-head fastened joint

The lap joint is made from two 57 × 135 mm 2024-T3 bare (ie. not Alclad) aluminium alloy sheets with a thickness of 1.016 mm (0.04 inch). The sheets were fastened together using six MS20470 AD4-5 dome-head fasteners with a shank diameter of 3.175 mm. This lap joint is being used by the authors in a number of studies, and is intended to be a very simple representation of joints found in skin structure of light (General Aviation) aircraft, in term of skin thickness, fastener type and fastener spacing. In order to contain the number of variables in this analysis, the joint is assumed to be unsupported ie. no underlying structural attachment is considered in this initial analysis. The presence of such substructure would add an additional variable in the form of joint eccentricity.

To scope the issue, the loading used in the analysis was high – the load capacities of the two joints were calculated based on four possible failure modes, namely fastener shear failure, sheet tension failure, sheet bearing failure and sheet tear out failure (see **Error! Reference source not found.**). The strength calculation [16] led to an estimated joint capacity (critical failure stress) of 169 MPa (corresponding to fastener shear). This value was adopted as applied tensile stress for the finite element analysis in this paper [1].

Further simplifications were that the analysis of the deformation of the aluminium substrate assumed elastic isotropy. The joint clamping force was approximated as equivalent to a torque of 7.91 Nm. This is an average value from the recommendation of a range of 6.78-9.04 Nm by Hi-Shear Corporation [17]. The coefficient of friction was assumed to be 0.2 for all faying surfaces around the joint [18]. Other research programs are assessing these variables as factors in joint performance, and will

[1] Noting that operating conditions for a joint should not normally exceed 2/3 of these extreme values

contribute to an improved model as results become available.

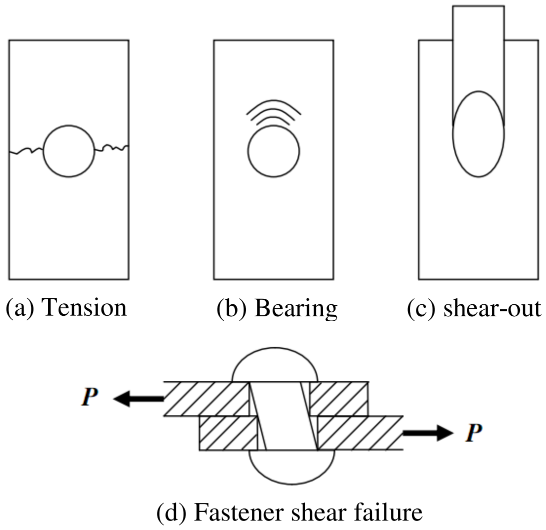

Figure 2 Common failure modes of structural joints

3.2 Countersunk Type Fastener

Another joint configuration assessed in this study is adapted from ref. [19]. The joint is made from two 50 × 200 mm 7475-T761 aluminium alloy sheets where the sheet thickness is 3 mm, fastened together using four countersunk fasteners. The fastener material is Ti-6Al-4V with a shank diameter of 6 mm and are installed with an interference fit of 50 micrometres using Hi-Lok nuts.

Countersunk fasteners are commonly used on the exterior of aircraft to maintain aerodynamic performance (minimising the drag). A countersink depth that produces 'knife-edge' conditions has been responsible for fatigue cracking in aircraft structures, and this places constraints on the sheet thicknesses suitable for such fastening; it is recommended that the thickness of the top (countersunk) sheet be at least 1.5 times the depth of the countersink [20].

In this case, the critical failure stress of the joint is calculated to be 191 MPa (with a failure mode of sheet tension), and again this high value was used in calculation.

4 Displacement Analysis

Under tensile loading, there was a propensity for the exposed sheet ends to open up, as illustrated in Figure 3 and Figure 4 for dome-head and countersunk lap joints. This out-of-plane movement, commonly known as secondary bending, occurred due to the presence of geometric eccentricities [21]. This phenomenon is detrimental to the fatigue properties of a joint, since it can give rise to significant changes in the stress concentration around fastener holes, assisting development of fatigue cracks at or near the stress concentration, and the bending can also introduce unwanted additional stress in fasteners.

The movement of the joint concentrates the applied strain into discrete locations such as the sheet ends, and this location was selected for the analysis. In a real structural joint, a fillet of sealant coat is often generated, squeezed out under pressure while the joint is being manufactured, as shown (for the dome fastener) in Figure 5. Assuming a 45° sealant bead and coating covering the exposed sheet ends in the lap joint, the effective length of the coatings is denoted as l^*. For this exercise, to minimize variable, no faying surface sealant was included in the model.

More specifically, for these particular geometries of dome-head fastened lap joint, the displacement calculated was between the upper (free) corner of the top sheet, and the point on the lower sheet where a 45 degree sealant bead meets the lower sheet. This displacement then allowed estimation of the strain in a paint film over sealant at the end of the joint. This model is an improved estimate relative to earlier work, in that the assumed sealant configuration allows the bending of the lower (loaded) sheet to be incorporated.

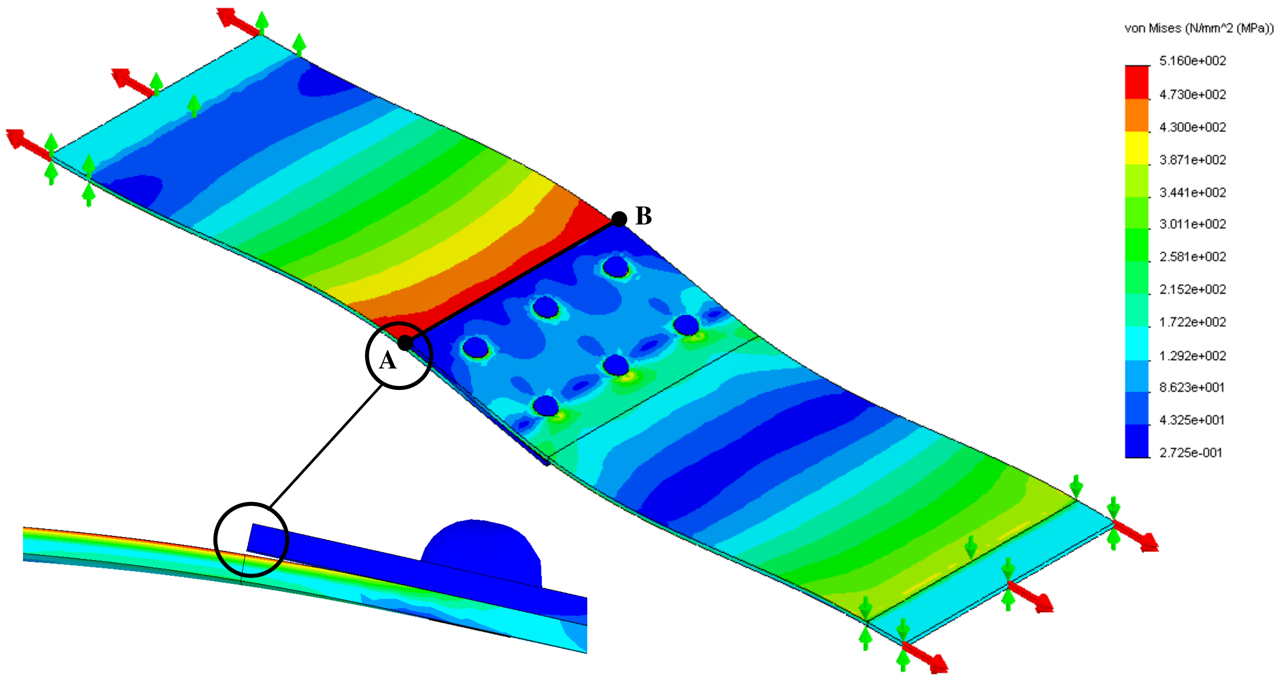

Figure 3 von Mises stress distribution and sheet ends opening up (for dome-head lap joint)

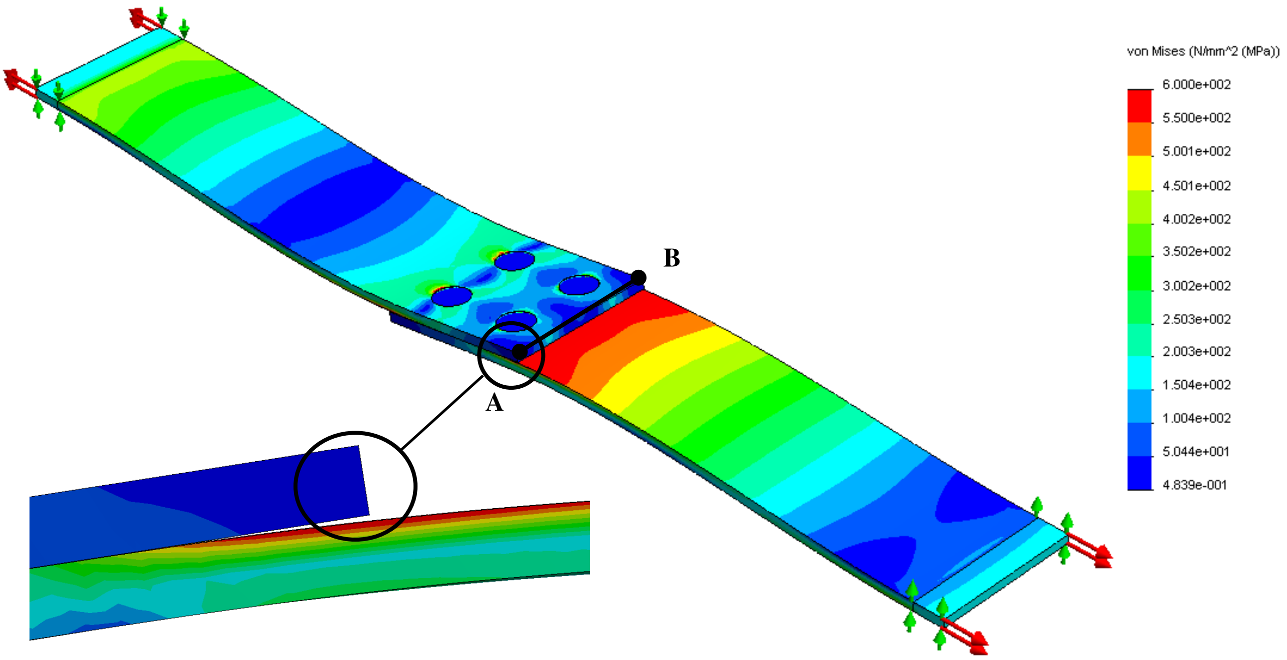

Figure 4 von Mises stress distribution and sheet ends opening up (for countersunk lap joint)

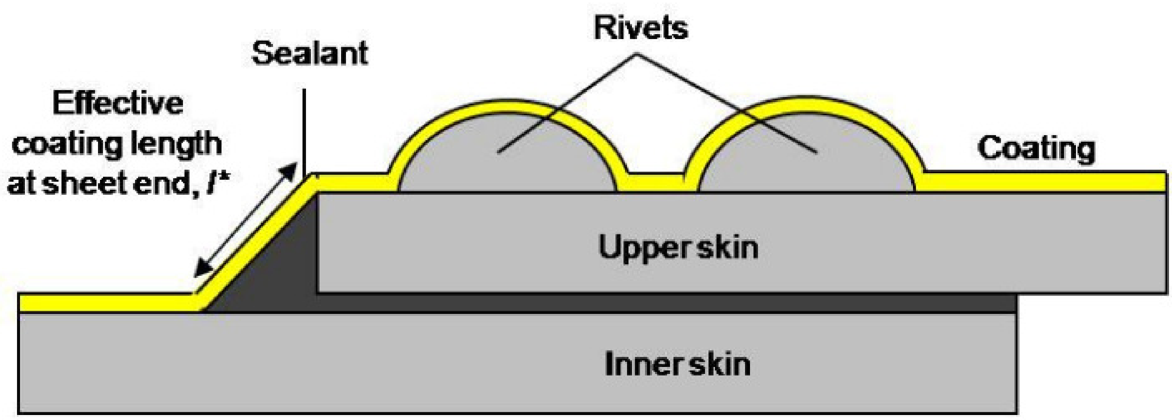

Figure 5 Effective length of coating covering lap joint sheet ends (dome-head type fastener). The strain predicted is along length *l**

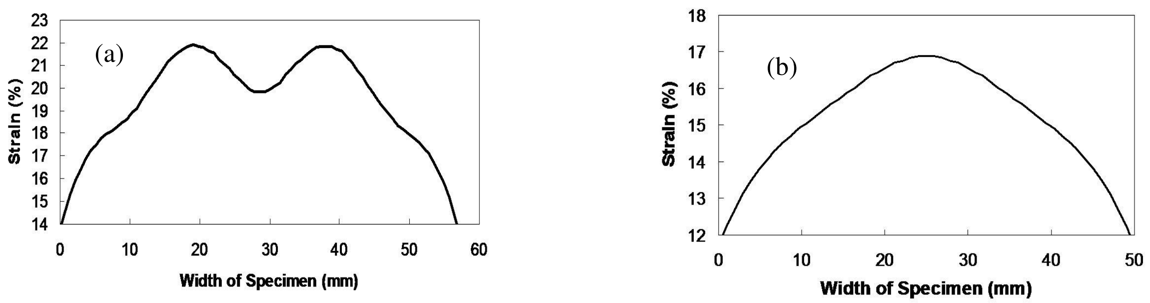

Figure 6 Strain distribution across the width of lap joint specimens at exposed sheet ends (a) dome-head lap joint (b) countersunk lap joint

The modelling results were as follows:

- **For the dome-head fastened joint, the maximum strain in the 45 degree sealant/paint bead was 21.9%**
- **For the countersunk fastened joint the maximum strain in the 45 degree sealant/paint bead was 16.9%**

Figure 6 illustrates an additional observation – the way that the strains in the bead at the exposed sheet ends vary across the width of the specimen (ie. from point A to B in Figure 3 and Figure 4 for the dome-head type and countersunk type fastener respectively). The maximum strain is found between fasteners, indicating that the effect of fastener clamping is a significant one, and will need to be factored in for future analyses.

It was observed that the out-of-plane displacement contributes significantly due to the effect of joint eccentricity; which causes rotation of the unloaded sheet end, and hence adds strain to the sealant at the sheet end. Future work will need to assess the effects of any additional substructure which would be expected to change the eccentricity, and lead to additional variation in displacement, depending on configuration.

5 Impact of Joint displacement on Coating Integrity

The maximum strain over the length of *l** of approximately 21.9% for the dome-head joint and 16.9% for the countersunk joint represent a significant strain concentration. For example, the mechanical strains experienced on, say, a flat sheet in the middle of the wing would be expected to be a small fraction of one percent.

The paint coating strains calculated here, however are higher than that likely to be experienced in service, since the analysis used the maximum joint capacity as loading, and structural integrity requirements demand operation at less than this. While the particular displacement discussed here involves secondary bending, and is therefore likely to exhibit some non-linearity with load, maximum operating strain values about two-thirds of the values calculated would probably be reasonable.

In this study, it is assumed that the coatings will fail or crack when this value exceeds the strain to failure of a representative coating material. Hegedus et al. [22] noted that although epoxy primers have relatively high tensile strength (>17MPa), they display poor elongation (<10%). This indicates the concentrated coating strain in both lap joints could quite conceivably exceed the critical strain to failure of a coating material.

Clearly, the condition of the coating will be significant – degradation under service environmental conditions is expected to make the coating far more susceptible to cracking and failure. In addition, the environmentally-induced degradation state and the strain-induced degradation state may well interact in the sense that early high loading, or early sever environmental exposure, might enhance the coating's sensitivity to the other degradation mechanism. In effect, the actual load and environment sequences experienced might change the coating life. This is additional to the issue of coating life being dependent on the coating experiencing a suitably high strain. The estimation of a representative thermomechanical load history is therefore an important issue in terms of developing a coating life prediction capability.

6 Concluding Remarks

This research is intended to explore the extent to which displacements in aircraft joints might be a factor influencing the longevity of aircraft coating system. The results from the study indicate:

i. The maximum displacement for a notional end-of-sheet sealant and paint bead, for both lap joints, was found to occur at a position between two adjacent fasteners along the joint line.

ii. Secondary bending was observed to be a significant contributor to the displacements at the joint sheet ends. This contribution is expected to vary with joint/substructure configuration.

iii. The displacement at the sheet ends for dome-head and countersunk type of lap joint is likely represent a coating strain of the order of 21.9% and 16.9% respectively at these high applied loads. In service, strains might approach two-thirds of this.

Although this study focused on coating performance at sheet ends, other stress concentration regions, such as around fastener head region, are expected to be critical as well. Future work will consider these locations and other aspects of the thermomechanical history effect, such as load sequence effect, cumulative damage estimation, interfacial adhesion strength, and residual stress; all of which may have significant roles in influencing the longevity of aircraft protective coatings.

Acknowledgement

The authors wish to acknowledge with gratitude financial support from the Defence Materials and Technology Centre in Melbourne, Australia. Technical inputs from Dr. Bruce Crawford of the Defence Science and Technology Organisation, DSTO, are greatly appreciated.

References

[1] Wanhill R J H. Corrosion and fatigue assessment of aircraft pressure cabin longitudinal lap splices. *NLR-TP-99408*, National Aerospace Laboratory, Amsterdam, 1991.

[2] Aloha Airlines, Flight 243, Boeing 737-200, N73711, near Maui Hawaii, April 28, 1988. NSTB/AAR-89/03, National Transportation Safety Board, Washington, D.C. 20594, 1989.

[3] Furuta S, Terada H and Sashikuma H. Fatigue strength of fuselage joint structures under ambient and corrosive environment. *ICAF'97: Fatigue in New and Aging Aircraft*. EMAS Ltd, pp 231-249, 1997.

[4] Clark G. Corrosion and the management of structural integrity. *Structural Integrity for the Next Millennium*. Warley: EMAS Ltd, 1999.

[5] Pappas S P. Weathering of coatings-formulation and evaluation. *Progress in Organic Coatings*, Vol. 17, No. 1, pp 107-114, 1989.

[6] Blakey RR. Evaluation of paint durability-natural and accelerated. *Progress in Organic Coatings*, Vol. 13, pp 279-296, 1985.

[7] Morrow A M, Allen N S and Edge M. Photodegradation of water-based acrylic coatings containing silica. *Journal of Coatings Technology*, Vol. 70, No. 880, pp 65-72, 1988.

[8] Bondzic S, Hodgkin J, Krstina J and Mardel J. Chemistry of thermal ageing in aerospace epoxy composite. *Journal of Applied Polymer Science*, Vol. 100, No. 3, pp 2210-2219, 2006.

[9] Feldman D. Polymer weathering: Photo-oxidation. *Journal of Polymers and Environment*, Vol. 10, No. 4, pp 163-173, 2002.

[10] Skaja A, Fernando D and Croll S. Mechanical property changes and degradation during accelerated weathering of polyester-urethane coatings. *Journal of Coatings Technology and Research*, Vol. 3, No. 1, pp 41-51, 2006.

[11] Guo X, Michaels C A, Drzal P L, Jasmin J, Martin D, Nguyen T and Martin J W. Probing photodegradation beneath the surface: a depth profiling study of UV-degraded polymeric coating with microchemical imaging and nanoindentation. *Journal of Coatings Technology and Research*, Vol. 4, no. 4, pp 389-399, 2007.

[12] Yang X F, Vang C, Tallman D E, Bierwagen G P, Croll S G and Rohlik S. Weathering degradation of a polyurethane coating. *Polymer Degradation and Stability*, Vol. 74, No. 2, pp341-351, 2001.

[13] Yang X F, Tallman D E, Bierwagen G P, Croll S G and Rohlik S. Blistering and degradation of polyurethane coatings under different accelerated weathering tests. *Polymer Degradation and Stability*, Vol. 77, pp 103-109, 2002.

[14] Popov A A, Rapoport N and Zaikov G. *Oxidation of stressed polymers*, Gordon and Breach Science Publishers, 1991.

[15] White J R and Turnbull A. Weathering of polymers: mechanisms of degradation and stabilization, testing strategies and modelling. *Journal of Materials Science*, Vol. 29, No. 3, pp 584-613, 1994.

[16] Pilkey W D. *Formulas for stress, strain and structural matrices*, John Wiley & Sons, Inc., 2005.

[17] Hi-Lok product specification 342, 100 flush shear head. *Alloy steel*, Hi-Shear Corporation, 1992.

[18] Atre A and Johnson W S. Analysis of the effects of interference and sealant on riveted lap joints. *Journal of Aircraft*, Vol. 44, No. 2, pp 353-364, 2007.

[19] Starikov R. Fatigue behaviour of mechanically fastened aluminium joints tested in spectrum loading. *International Journal of Fatigue*, Vol. 26, pp 1115-1127, 2004.

[20] Park C Y and Grandt A F. A proposed fatigue test protocol for generic mechanical joints. *Engineering Failure Analysis*, Vol. 13, pp 136-154, 2006.

[21] Schijve J and Campoli G and Monaco A. Fatigue of structures and secondary bending in structural elements. *International Journal of Fatigue*, Vol. 31, pp 1111-1123, 2009.

[22] Hegedus C R, Spadafora S J, Pulley D F, Eng A T and Hirst D J. Chater 58 - Aerospace and aircraft coatings. *Paint and coating testing manual*, ASTM International, 1995.

Copyright Statement